
MICRO-FTIR SPECTROSCOPY CHARACTERIZATION OF MONUMENTAL STONES PROTECTIVE COATINGS

**Bogdana Simionescu^{*}, Mihaela Olaru, Magda Aflori and
Florica Doroftei**

*Petru Poni Institute of Macromolecular Chemistry, 41 A Gr. Ghica Voda Alley, 700487, Iasi,
Romania*

(Received 7 December 2010, revised 17 February 2011)

Abstract

Total reflection Fourier transform infrared (ATR-FTIR) spectroscopy was used to assess the effectiveness of four polymeric hydrophobic coatings in the conservation of two monumental stones, originating from Spain and Romania. The selected coatings include three commercially available siloxane-based water repellent products, as well as a new hybrid nanocomposite with silsesquioxane units synthesized *via* the sol-gel technique. Micro-FTIR analyses were performed in order to chemically monitor the distribution of the chemical treatments within the treated stones by obtaining a chemical map of the siloxane-based water repellent treatments within the limestone's cross-sections.

Keywords: micro-FTIR, siloxane-based water repellent, limestone, nanocomposite

1. Introduction

Fourier-transform infrared (FTIR) microscopy is a modern analytical technique enabling molecular imaging of a complex sample in the mid-IR range. With this technique, based on the absorption of IR radiation by vibrational transitions in covalent bonds, unique images with high spatial resolution can be obtained. Unlike conventional FTIR spectroscopy, which employs a single detection element, FTIR imaging enables spectroscopic and spatial information to be obtained simultaneously over a given field. FTIR imaging has been used to investigate a wide variety of materials, ranging from polymers [1-3] to biological samples [4-7], pharmaceuticals [8] and forensics [9]. While FTIR spectroscopic imaging was used since 1995 [10], it has only recently been applied to conservation science [11]. Thus, Spring et al. [12] used the ATR-FTIR imaging for the investigation of the chemical components of paint cross-sections from old master paintings. A recent application in Earth sciences of single spot analysis has been reported by Castro et al. [13], a correlation between the distribution of hydroxyl groups surrounding the spherulites and the expulsion

^{*} E-mail: simionescubogdana@yahoo.com

of water during crystallization of an anhydrous mineral assemblage replacing the spherulite glass being established. Ricci et al. have reported the potential of micro-ATR-FTIR spectroscopic imaging as a promising new method with high spatial resolution for the study of nineteenth and twentieth century albumen photograph cross-sections [14].

There are several advantages of using the micro-FTIR technique for minerals analysis. The sample size required to obtain good spectra is minimal (sub-milligram quantities). Moreover, the technique is sensitive to certain common minerals and may provide a quick approach to distinguish polymorphs - minerals with the same chemical composition, but with a different crystal structure. Micro-FTIR is also useful as a complementary or alternative technique to other more traditional methods as scanning electron microscopy (SEM) with energy dispersive spectroscopy (EDX). While a mineral specimen may take several hours to be analyzed by XRD, micro-FTIR technique can produce a spectrum unique to a mineral in a few minutes. Kaolinite is often cited in the literature as an example of a mineral which when present as a minor impurity may be more difficult to detect by X-ray analysis than by FTIR [15].

In this research, two carbonate rocks, originating from Spain and Romania, were used. Among all existing rocks, the carbonate ones have a special significance, due to their abundance and economic value. This type of rocks is the most used as building material for stone monuments, especially for their physical/mechanical properties (durability/resistance). People representing cultures around the world are using limestone to build monuments for thousands of years: the Egyptian pyramids, London's Saint Paul's Cathedral, Empire State Building in New York are just a few examples of the limestone usage spreading all over the world. Some criteria were taken into account for stones' selection: two limestones were selected in order to be comparable but, at the same time, the stones present different properties and characteristics, leading to different behaviours after the application of the chemical products and performing of durability tests, as well. Other aspects that were taken into consideration in the selection of the materials were their regional/national significance and availability, as well as their level of usage as building materials for the construction of buildings which present historic and artistic importance and have a cultural significance.

The first selected rock is a micritic dolomitic limestone, called Laspra, originating from northern Spain, Asturias. In historical references, Laspra's quarry is mentioned under the name of Laspra (1451) and Aspra (1463), and also Amilladoiro (1473), Omilladoiro (1493), and Milladoiro (1505). This rock was widely found in Asturias, especially in the surroundings of Oviedo, being used, for example, as one of the three building materials of the San Salvador Cathedral of Oviedo (1293-1587) [16]. Inner parts of two pre-romanesque churches from the IXth century near Oviedo, named Santa Maria del Naranco and San Miguel de Lillo were also built using Laspra [16]. These two small churches are listed in UNESCO's Heritage List since 1985. Oviedo's Cathedral is one of the most characteristic buildings of the late gothic architectural style in the region of

Asturias and presents a significant interest since it reflects all gothic style evolution in Spain. San Salvador Cathedral was the first gothic monumental building constructed in Asturias. The other chosen limestone is coming from Romania and is a bioclastic oolitic stone, named Repedea. The limestone may be found in the eastern part of Romania, along the Moldavian Platform. In this area, Repedea is the main building material used for the construction of important churches and especially monasteries, since antiquity until nowadays, the most representative churches/monasteries in this part of the country being built, in most of the cases, only from Repedea. An exemple is Dobrovat monastery, which has an important cultural and historical value; the whole monastery assembly was built between 1503 and 1504 [16].

The present study is aimed to use micro-FTIR microscopy in reflection mode (ATR) to chemically monitor the distribution of different polymeric coatings in order to investigate their efficiency in stone conservation. Three of the applied coatings are commercially available siloxane-based oligomers and polymers and one is a new hybrid nanocomposite with silsesquioxane units [17] synthesized *via* sol-gel technique in order to be used for the same purpose as the commercial ones. This investigation method enabled the semi-quantitative quantification of the presence of siloxane-based water repellents due to the appearance of characteristic vibration bands of silicate groups and the estimation of the efficiency of the newly synthesized nanocomposite material (TMSPMA). The elemental maps recorded using EDX analysis in an environmental scanning electron microscope (ESEM-EDX) together with backscattered electron images from the ESEM were additionally used to confirm the composition and morphology of each chemical product.

2. Experimental

2.1. Materials

The worldwide used siloxane-based chemical products which have been tested in the present study are: (1) Lotexan-N (Keim), a siloxane prepolymer substituted with methoxy, methyl and alkyl groups dissolved in a mixture of aromatic/aliphatic hydrocarbon solvents; (2) Silres BS 290 (Wacker), a mixture of silanes and siloxanes, applied using white spirit as solvent and (3) Tegosivin HL 100 (Goldschmidt-Degussa), a typical siloxane resin having ethoxy and methyl substituents attached to silicone atoms, mixed with white spirit as solvent. The hybrid nanocomposite with silsesquioxane units (TMSPMA) was obtained through a combination between the sol-gel technique and the radical polymerization of an alkoxy silane sol-gel precursor, 3-(trimethoxysilyl)propyl methacrylate, in the presence of a primary amine surfactant [17].

2.2. Characterization

Fourier-transform infrared (FTIR) microscopy and EDX analysis in an environmental scanning electron microscope (ESEM-EDX) together with backscattered electron images from the ESEM were used in order to gather information on stone minerals composition, as well as on stone – polymer interactions. A Nicolet Continuum FTIR microscope was used in reflection mode with a micro slide-on ATR (Si crystal) device or in transmission mode with a diamond anvil cell on some particles. The FTIR microscope was equipped with a MCT (Mercury Cadmium Telluride) detector cooled by liquid nitrogen and a 15 x Thermo-Electron Infinity Refflachromat objective with a tube factor of 10x. Spectra from 4000 to 650 cm^{-1} (ATR/ diamond cell) have been registered with a FTIR Thermo Nicolet Avatar 370, at a resolution of 4 cm^{-1} and a mirror velocity of 1.8988 $\text{cm}\cdot\text{s}^{-1}$. A total of 64 scans have been recorded and the resulting interferogram averaged. Acquisition and post-run processing have been carried out using Nicolet ‘Omnic’ software. The ESEM micrographs were obtained with a Quanta 200 scanning probe microscope, the specimens being fixed with adhesive past on cylindrical-shaped Al conducting supports and then sputtered-coated with gold. The microscope was equipped with an Oxford Inca Energy Dispersive X-ray (EDX) system for chemical analysis, elemental analysis mapping and linescans.

3. Results and discussion

After embedding the limestone samples in polyester resin and polishing them in cross-section, the investigation of the water repellents distribution within the cross-sectioned samples was performed through microFTIR-ATR and ESEM-EDX measurements. From the microscopic point of view, Laspra presents a microcrystalline texture and is composed mainly of dolomite, calcite and ankerite with micritic grain size, as well as of small amounts of quartz. In some areas, the stone presents microsparitic grain size along the pores [18]. The frequency assignments reported by Hertzberg et al. [19] for carbonate minerals are an symmetric stretching ν_1 (infrared inactive, its presence being correlated with a disorder in the symmetry of carbonate group), an out-of-plane bending ν_2 (909-833 cm^{-1}), a doubly degenerate asymmetric stretching ν_3 (1420-1480 cm^{-1}), the in-plane-bending ν_4 (769-666 cm^{-1}) and the combination modes ($\nu_1+\nu_3$) and ($\nu_1+\nu_4$). Figure 1 shows the FTIR spectrum of an area of a cross-sectioned Laspra sample treated with Tegosivin HL 100. In this spectrum, the bands located at 1443, 882 and 728 cm^{-1} can be attributed to CO_3^{2-} anion originating from the dolomite [20]. Calcite bands are not seen because there are located at similar frequencies as the dolomite (1428, 878 and 714 cm^{-1}) and therefore overlapped with the bands of this predominant mineral. Even though quartz is a minor constituent, it can be clearly identified through the bands located at 1144, 790 and 780 cm^{-1} , attributed to SiO_4 group vibrations. The band located at 1040 cm^{-1} can be associated only with the silicate groups from Tegosivin HL 100.

The micrographs of cross-sectioned samples treated with the siloxane-based compounds showed, from the chemical point of view, the localization of the water repellent treatments within the 1 cm in depth cross-sectioned limestone samples, a few images being presented below. Figure 2 shows, as an example, a micrograph of a Laspra sample which was treated with Tegosivin HL 100, embedded in resin, polished and then submitted to the experiment.

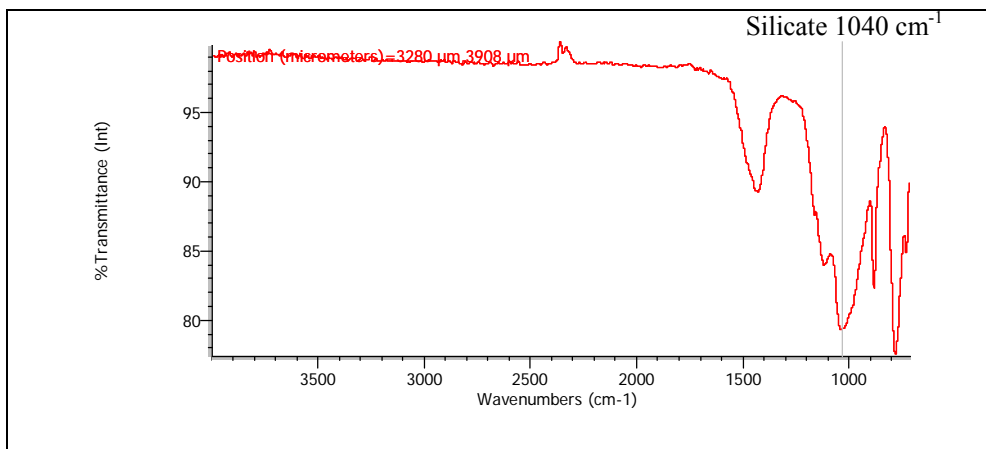


Figure 1. Silicate FTIR spectrum of an area of a cross-sectioned Laspra sample treated with Tegosivin HL 100.

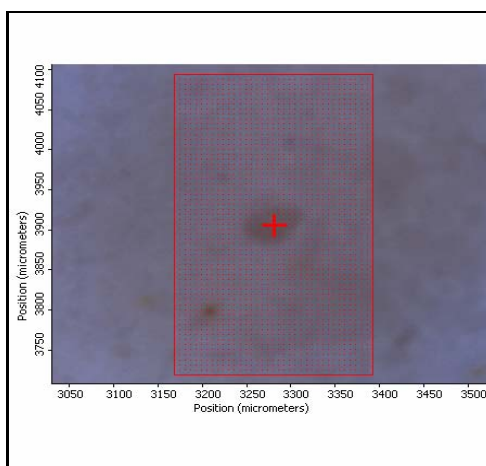


Figure 2. Micrograph of an area of a cross-sectioned Laspra sample treated with Tegosivin HL 100.

The micrograph illustrates the presence of a huge pore (pore size of about 65 x 34 micrometers) roughly situated in the middle of the selected area. In the additional chemical map (Figure 3) one can distinguish the intensities of the silicate band, corresponding to the siloxane-based product (Tegosivin HL 100). The signal of the band corresponding to the silicate is gradually decreasing from

red (high intensity of the silicate band) to yellow, green and blue (very low to no intensity of the silicate band).

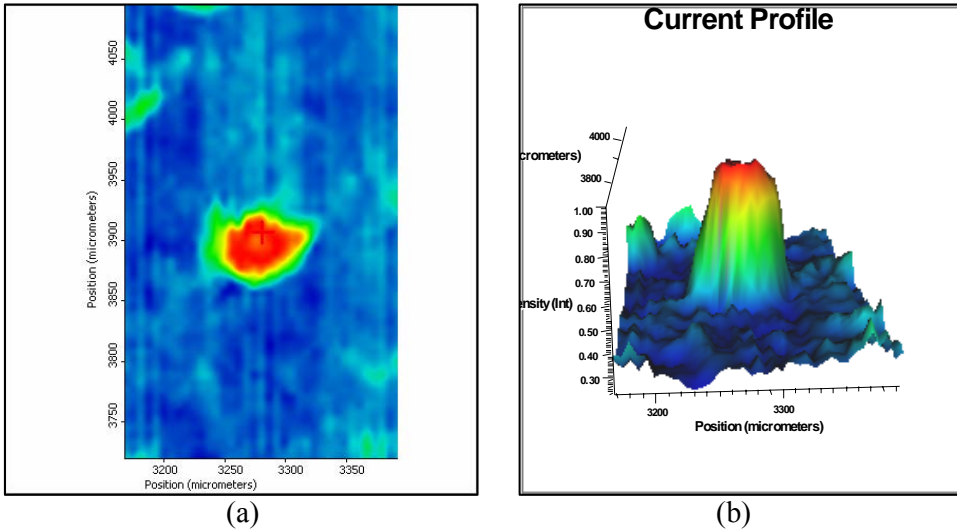


Figure 3. Chemical map of an area of a cross-sectioned Laspra sample treated with Tegosivin HL 100. (a) 2D map; (b) 3D map showing the intensity of the silicate treatment.

Figure 3 shows that the highest intensity of the band corresponding to the water repellent silicate can be found within the pore, gradually decreasing towards pore's rims. This is a clear indication of the fact that the siloxane-based treatments are concentrated, even after solvent's evaporation, in stone's larger pores, coating and filling them and, therefore, blocking and disabling these stone areas to 'breathe'. The majority of researchers involved in conservation science agree that the stones need to 'breathe', meaning that the stone should remain permeable to water vapour, in order to avoid any buildup of moisture at the interface between the treated zone and the untreated stone below. The filling of the pores with a chemical treatment usually means also the formation of additional pressures between the surfaces, leading to cracks or fissures. These worldwide used siloxane-based chemical products proved to have a poor resistance to salt mist accelerated ageing and SO₂ dry deposition [21, 22] and one reason for these drawbacks could be correlated with the blocking of the stone's larger pores.

To obtain additional information on the distribution of the siloxane-based water repellent treatments within the two porous stones, this technique was correlated with the samples mapping which can be achieved through the SEM-EDX technique.

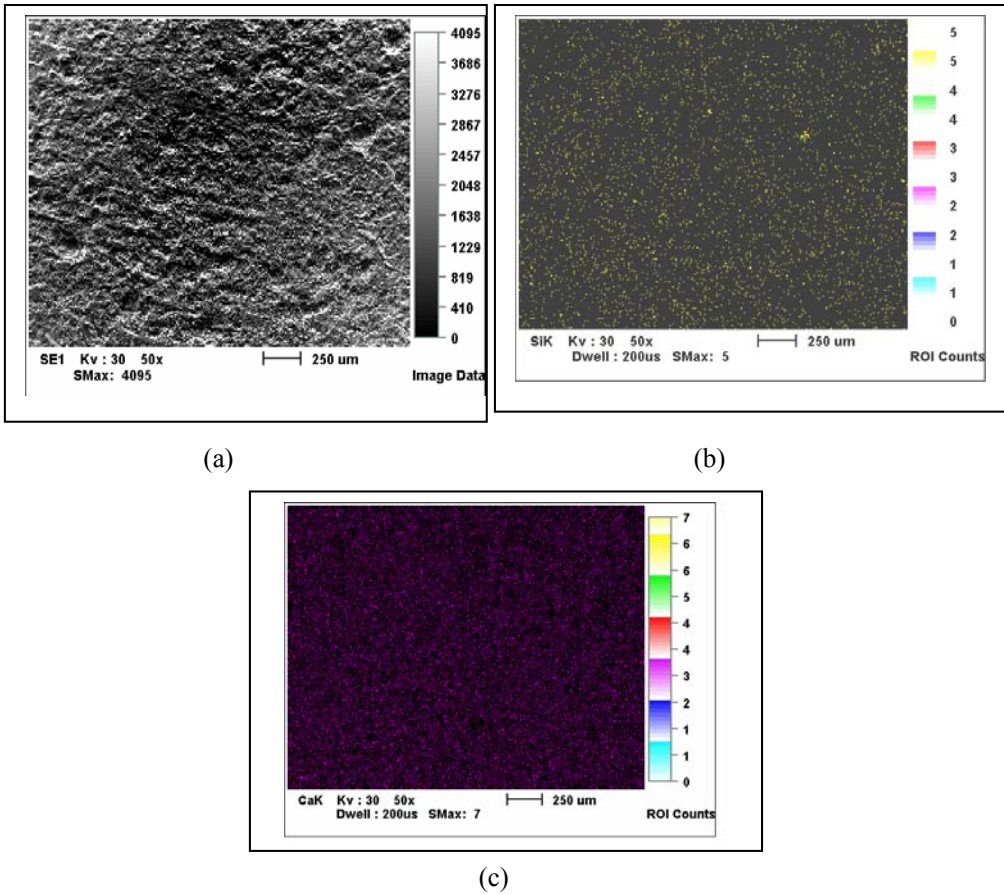


Figure 4. Mapping of an area of a Lapra sample treated with Tegosivin HL 100: (a) SEM micrograph; (b) EDX mapping showing in yellow the Si distribution; (c) EDX mapping showing in purple the Ca distribution.

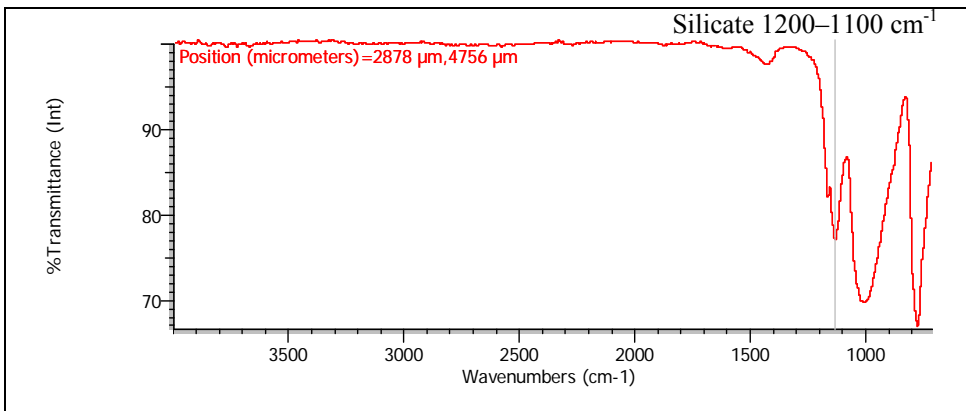


Figure 5. Silicate FTIR spectrum of an area of a cross-sectioned Repedea sample treated with Lotexan-N.

It has to be mentioned that using the EDX mapping technique one can obtain a map corresponding to the localization of different chemical elements on a certain sample, but not a chemical map, this technique being unable to distinguish if the detected chemical element (e.g., Si) belongs to stone's minerals or to the applied chemical treatment. A typical EDX mapping (silica, calcium) for the cross-sectional area of Laspra limestone samples is shown in Figure 4.

The same techniques were applied for all Repedea treated samples. Repedea's texture can be described as an oolitic grainstone. The stone's matrix, between the oolites, is a micritic and microsparitic one, containing mainly calcite, magnesian calcite, quartz and aragonite. Figure 5 shows the FTIR spectrum of an area of a cross-sectioned Repedea sample treated with Lotexan-N.

In this spectrum, the bands located at 1430 and 795 cm^{-1} can be attributed to CO_3^{2-} anion originating from calcite (1430 cm^{-1} - asymmetric stretching vibrations of carbonate, 795 cm^{-1} - in-plane bending vibrations of carbonate ion) [20]. Silica (quartz) bands can be observed at 1168 cm^{-1} , 1004 cm^{-1} , while the doublet originating from Si-O-Si bending vibrations that normally appears at 798-779 cm^{-1} is overlapping with the in-plane bending vibrations of carbonate ion. The band located at 1140 cm^{-1} can be associated only with the silicate groups from Lotexan-N.

Figure 6 illustrates a micrograph representing a small part of a Repedea treated with Lotexan-N cross-sectioned sample. In the centre of the image one can observe the presence of an almost perfectly rounded oolite surrounded by voids. The corresponding chemical maps are shown in Figure 7.

As in the case of Laspra cross-sectioned sample treated with Tegosivin HL 100, the chemical maps are clearly illustrating that the silicate belonging to the siloxane-based water repellent product registers a higher intensity of the band localized in stone's pores surrounding the oolite, the intensity decreasing from red to yellow, green and blue. From this chemical map it again appears that the silicate treatment is coating and filling Repedea's pores – the absence of any intensity corresponding to the treatment's silicate band in the oolite area being explained by the fact that the intensities of the carbonate band are extremely strong, shadowing or overpowering the lower intensities corresponding to the silicate band.

The EDX mapping of a Repedea sample treated with Lotexan-N is shown in Figure 8. The monitorization of the distribution of the commercially available products within the treated limestone samples has demonstrated that all three products manifest the same behaviour in relation to stone's substrates, no significant difference being registered among the distribution of Lotexan-N, Silres BS 290 and Tegosivin HL 100 within Laspra or Repedea samples.

The same techniques were used to monitor the localization of the newly synthesized water repellent nanocomposite within Laspra and Repedea cross-sectioned samples.

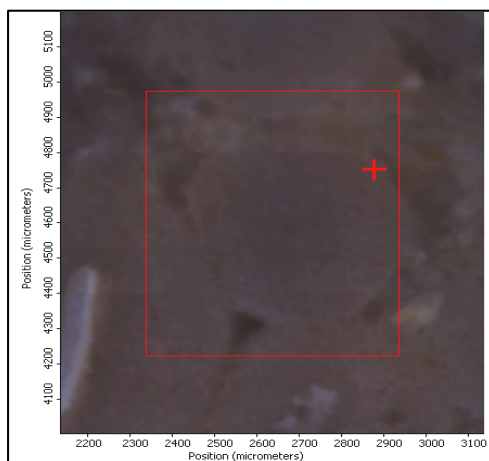


Figure 6. Micrograph of an area of a cross-sectioned Repedea sample treated with Lotexan-N.

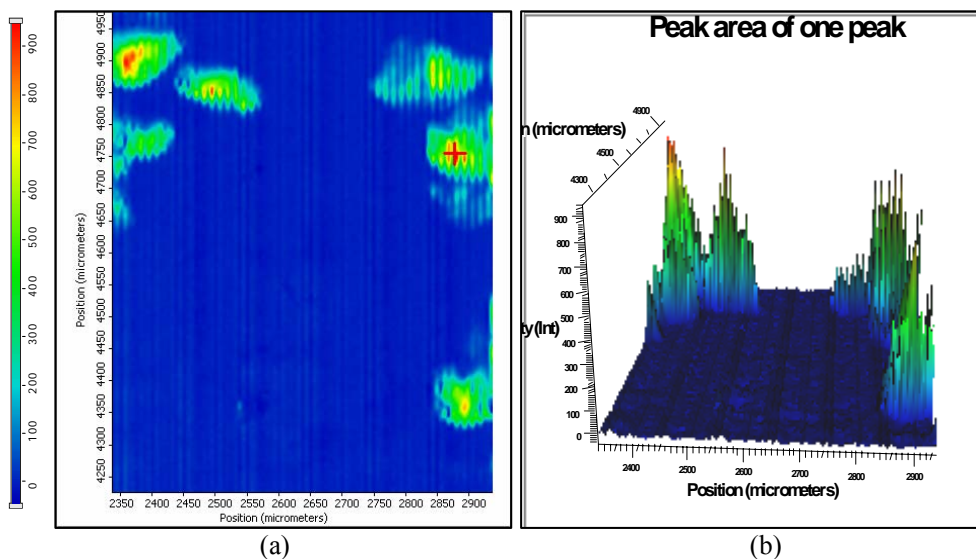


Figure 7. Chemical map of an area of a Repedea sample treated with Lotexan-N: (a) 2D map; (b) 3D map showing the intensity of the silicate treatment.

The performance of micro-FTIR-ATR technique on TMSPPMA treated Laspra and Repedea samples (cross-section) yielded no results – the chemical maps, performed repeatedly, illustrate the complete absence of the intensities corresponding to TMSPPMA’s silicate bands. Since both limestone samples were treated with the nanocomposite material before their preparation for the microFTIR-ATR investigation, one can conclude that the nano-dimensioned silicate particles of the treatment determined a localization and distribution of TMSPPMA impossible to be detected using this technique, which can function

within the micrometer and not nanometer range. Due to the self-assembling properties, the nano-builder (TMSPMA precursor) introduces particular atoms and molecules into limestone's structure. The molecules then align themselves into particular positions, forming a variety of intermolecular, weak forces in order to minimize the system's total energy.

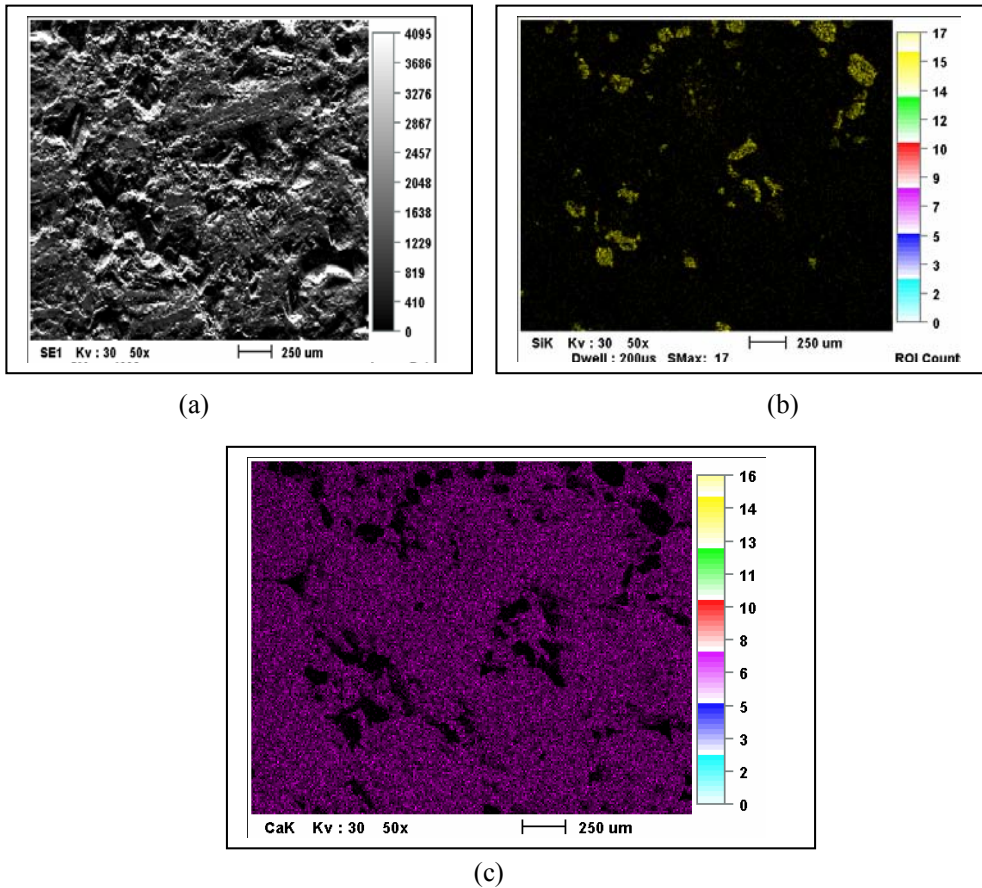


Figure 8. Mapping of an area of a Repedea sample treated with Lotexan-N: (a) SEM micrograph; (b) EDX mapping showing in yellow the Si distribution; (c) EDX mapping showing in purple the Ca distribution.

Over the curing period, silsesquioxane nanoparticles self-assemble and bond to the stone's surface, the nanocoating remaining not only at the stone's surface, but deeply penetrating the inner stone's structures without blocking the stone's pores due to the hybrid nanocomposite's structure (nano-sized particles and self-assembling properties). As compared to the worldwide used products, the hybrid nanocomposite with silsesquioxane units was proved to represent the best choice for the protection of the limestones against salt mist action and SO₂ dry deposition since it showed a better water vapour permeability value, a

reducing of the sulphating degree at the surface and did not alter the colour of the stone samples [21, 22].

Distribution maps corresponding to the nanocomposite product's localization in Laspra and Repedea samples were obtained using EDX mapping (Figure 9). Figure 9 (b) shows the even distribution of the Si particles all over the selected area, which comes as opposite to the same maps performed on both Laspra and Repedea samples when treated with any of the commercial products. This can be also explained through the difference in composition, particle size, polymeric network arrangement and properties which are evident for the commercial compounds as compared to the nanocomposite material.

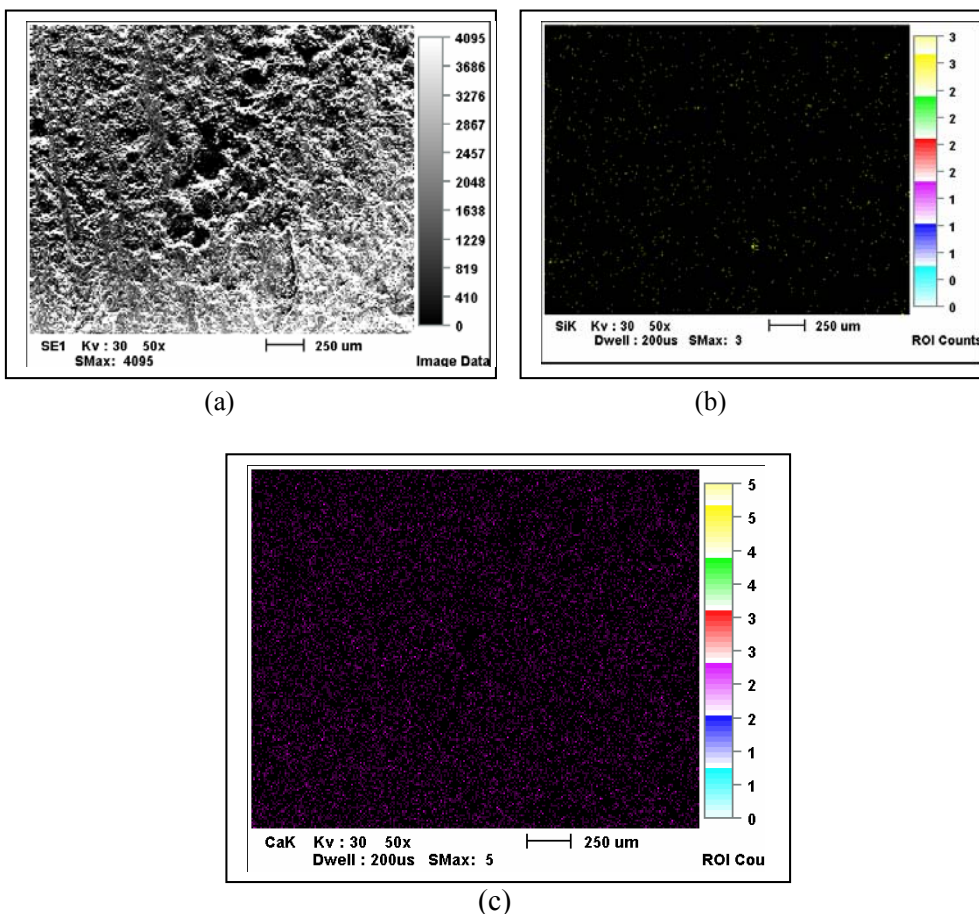


Figure 9. Mapping of an area of a Laspra sample treated with TMSpMA. (a) SEM micrograph; (b) EDX mapping showing in yellow the Si distribution; (c) EDX mapping showing in purple the Ca distribution.

4. Conclusions

The results of this research highlighted the feasibility and the relevance of micro-FTIR spectroscopy imaging in providing information on the effectiveness of the conservation of monumental stones at microscale using different protective coatings. As follows, this technique has been successfully used to identify silicate components belonging to water-repellent products within limestone treated samples. Moreover, by means of silicate mapping, it was possible to discriminate which applied coating proved to be more efficient from stone protection point of view. The commercially available siloxane-based mixtures of oligomers and polymers were shown to coat and fill the larger pores, blocking them and disabling the stones to breathe, while TMSPMA nanocomposite deeply penetrated the inner stone's structures without blocking the stone's pores due to nanocomposite hybrid's structure, this being proven, from the chemical perspective, using micro-FTIR spectroscopy.

Acknowledgements

One of the authors (B.S.) acknowledges the financial support of European Social Fund – ,Cristofor I. Simionescu' Postdoctoral Fellowship Programme (ID POSDRU/89/1.5/S/55216), Sectoral Operational Programme Human Resources Development 2007 – 2013.

References

- [1] O.S. Fleming, K.L.A. Chan, and S.G. Kazarian, *Polymer*, **47** (2006) 4649.
- [2] J.L. Koenig and J.P. Bobiak, *Macromol. Mater. Eng.*, **292** (2007) 801.
- [3] A. Gupper, P. Wilhelm, M. Schmied, S.G. Kazarian, K.L.A. Chan and J. Reussner, *Appl. Spectrosc.*, **56** (2002) 1515.
- [4] K.L.A. Chan, S.G. Kazarian, A. Mavraki and D.R. Williams, *Appl. Spectrosc.*, **59** (2005) 14.
- [5] D. Faibish, A. Gomes, G. Boivin, I. Binderman and A. Boskey, *Bone*, **36** (2005) 6.
- [6] K. Verdelis, M.A. Crenshaw, E.P. Paschalis, S. Doty, E. Atti and A.L. Boskey, *J. Dental Res.*, **82** (2003) 697.
- [7] C. Ricci, K.L.A. Chan and S.G. Kazarian, *Appl. Spectrosc.*, **60** (2006) 1013.
- [8] K.L.A. Chan and S.G. Kazarian, *Lab. Chip.*, **6** (2006) 864.
- [9] C. Ricci, S. Bleay and S.G. Kazarian, *Anal. Chem.*, **79** (2007) 5771.
- [10] E.N. Lewis, P.J. Treado, R.C. Reeder, G.M. Story, A.E. Dowrey, C. Marcott and I.W. Levin, *Anal. Chem.*, **67** (1995) 3377.
- [11] J. Van der Weerd, H. Brammer, J.J. Boon and R.M.A. Heeren, *Appl. Spectrosc.*, **56** (2002) 275.
- [12] M. Spring, C. Ricci, D.A. Peggie and S.G. Kazarian, *Anal. Bioanal. Chem.*, **392** (2008) 37.
- [13] J.M. Castro, P. Beck, H. Tuffen, A.R.L. Nichols, D.B. Dingwell and M.C. Martin, *Am. Mineral.*, **93** (2008) 1816.
- [14] C. Ricci, S. Bloxham and S.G. Kazarian, *J. Cult. Herit.*, **8** (2007) 387.
- [15] A.M. Awwad, R. Ahmad and H. Alsyouri, *Jordan J. Earth and Env. Sci.*, **1** (2009) 68.

- [16] B. Simionescu and M. Olaru, *Eur. J. Sci. Theol.*, **5(1)** (2009) 59.
- [17] B. Simionescu, M. Olaru, M. Aflori and C. Cotofana, *High Perform. Polym.*, **22** (2010) 42.
- [18] B. Simionescu, M. Aflori and M. Olaru, *Construct. Build. Mater.*, **23** (2009) 3426.
- [19] G. Herzberg, *Molecular spectra and molecular structure II. Infrared and Raman spectra of polyatomic molecules*, D. Van Nostrand, New York, 1945, 658.
- [20] M.J.A. Wilson, *A handbook of determinative methods in clay mineralogy*, Blackie & Son Ltd., New York, 1987, 308.
- [21] B. Simionescu, F. Doroftei, M. Olaru, M. Aflori and C. Cotofana, *J. Opt. Adv. Mater. – Symp.*, **1** (2009) 1077.
- [22] M. Olaru, M. Aflori, B. Simionescu, F. Doroftei and L. Stratulat, *Materials*, **3** (2010) 216.